

Extrinsic photoemission and diffusion of "free" excitons in solid xenon

Zohar Ophir, Nikolaus Schwentner, Baruch Raz, Michael Skibowski,* and Joshua Jortner†

Department of Chemistry, Tel-Aviv University, Tel-Aviv, Israel
and Sektion Physik der Universität München, München, Germany
(Received 27 December 1974)

Extrinsic photoemission from pure solid rare gases at energies below the direct photoemission threshold is assigned to the diffusion of "free" mobile excitons (prior to exciton trapping) to the gold (emitter) substrate followed by exciton-enhanced electron ejection from the electrode. From a semiquantitative study of the extrinsic photoemission yield of solid Xe as a function of the film thickness we get the diffusion length $l \approx 300$ Å, for exciton migration on the time scale of 10^{-11} – 10^{-12} sec.

Some of the most interesting features of exciton states in molecular crystals involve electronic energy transfer by excitons.¹ There have been extensive studies of the dynamics of Frenkel type singlet and triplet excitons in organic crystals and in polymers,^{2–8} resulting in the exciton diffusion length l which together with the exciton effective lifetime τ (which includes both radiative and nonradiative decay channels) give the exciton diffusion coefficient D . These data for exciton dynamics in organic crystals, obtained at moderately high temperatures, correspond to incoherent, diffusive type, motion of excitons, which are strongly coupled to the lattice phonons.^{1b,9} It is interesting to inquire whether similar dynamic information can be obtained for Wannier, hydrogenic type excitons (characterized by a principal quantum number $n \geq 2$) or for intermediate type $n = 1$ excitons¹⁰ in simple insulators, such as solid rare gases. Apart from intrinsic interest in extension of studies on exciton dynamics to new systems, the "simple" insulators mentioned above are of considerable interest in view of the ultrashort lifetime of mobile excitons in these solids. The vacuum ultraviolet optical emission spectra of pure solid Ar, Kr, and Xe exhibit the emission from the electronically excited, vibrationally relaxed, rare gas homonuclear diatomic molecules.¹¹ As no luminescence could be observed from "free" exciton states,¹¹ we conclude that efficient exciton trapping occurs on a time scale τ , which is short relative to radiative lifetime τ_r , i. e., $\tau \leq 10^{-2}\tau_r$. As $\tau_r \approx 10^{-9}$ sec, as inferred from the integrated oscillator strength for the $n = 1$ transition,¹² $\tau \approx 10^{-11}$ – 10^{-12} sec. The trapped exciton is practically immobile in view of small polaron effects. The "free" excitons¹³ can migrate in pure rare-gas solids and it will be interesting to gain physical information pertaining to exciton dynamics on the picosecond time scale in these systems. In this context, we have recently studied¹⁴ exciton induced photoemission resulting from exciton induced Auger type ionization of atomic and molecular impurities by $n = 1$ ($^2P_{3/2}$) "free" excitons, which result in the following diffusion lengths for these "free" excitons: $l = 170$ Å for pure solid Xe at 30 °K^{14a,15} and $l = 120$ Å for pure solid Ar at 20 °K.^{14b,14c}

We would like to propose that pertinent data on exciton dynamics in pure solid rare gases can be obtained from extrinsic photoemission data at energies below the direct photoemission threshold. In this article we present

the results of a study of extrinsic photoemission from solid Xe, which are assigned to exciton diffusion to a gold substrate followed by electron ejection from the electrode. These experiments provide a new method to determine exciton diffusion lengths in solid rare gases.

Intrinsic photoemission from pure^{14,16–18} solid rare gases is exhibited at energies $E_{th} = E_G - V_0$, where E_G is the interband threshold while V_0 corresponds to the energy of the bottom of the conduction band relative to the vacuum level. It is now empirically well established^{14,16–18} that all pure solid rare gases exhibit extrinsic photoemission following excitation in the excitonic region at energies below the threshold energy E_{th} . This extrinsic photoemission exhibits a pronounced structure in the excitonic region. Several possible interpretations of this effect should be considered:

(a) Exciton enhanced impurity ionization.¹⁶ Our recent results for doped crystals¹⁴ using ultrapure samples (impurity content not exceeding 1 ppm) and controlled doping conditions, seem to rule out this possibility.

(b) Nonlinear processes such as collisions between two "free" excitons,¹⁹ nonradiative long range coupling between a pair of localized excited diatomic molecules, or a (one-photon) photoionization process of a free exciton²⁰ or of a trapped excited diatomic molecule. These interesting processes are improbable under the condition of weak light intensities employed in such photoemission studies. These mechanisms can be definitely ruled out as the photoemission quantum yield is independent of the light intensity.¹⁴

After eliminating possible bulk effects we have to focus attention on the role of interphases, bearing in mind that such photoemission studies are conducted on thin films, which are mounted on a metal (in our case gold) emitter electrode. The following additional mechanisms should be considered:

(c) Ionization of excitons at the insulator–vacuum interface.²¹ Although our current understanding of surface states of insulators is meager it should be noted that the energy of the lowest $n = 1$ exciton in solid Xe is located at the energy 1.2 eV below E_{th} and 0.8 eV below E_G while for other rare gases these energy values are even higher, and it is difficult to conceive how the surface states of an insulator can overcome this large energy gap required for decay by ionization. Furthermore,

such a mechanism will imply that the yield for the extrinsic process is independent of the film thickness d , at least when d is sufficiently large to form a uniform layer. Our results, reported herein, demonstrate a strong d dependence of the yield and thus this mechanism can be safely rejected.

(d) Energy transfer (ET) from a localized, excited, diatomic molecule to the gold substrate, resulting in electron ejection from the gold. This mechanism can be described in terms of a (second order) nonradiative process where the donor molecule undergoes a bound-continuum transition which is accompanied by ionization of the acceptor, i. e., the metal film. This process bears a close analogy to the Forster-Dexter²² mechanism. Kuhn *et al.*²³ have utilized a similar process to study the quenching of low electronically excited molecular states by energy transfer to a gold substrate involving interband excitation in the metal.

(e) Exciton diffusion (ED) to the gold substrate followed by electron ejection from the electrode.^{14a} "Free," mobile excitons have to participate in this process which thus takes place on the time scale $t \sim \tau$. The energy transfer from the "free" exciton to the metal near the metal-insulator interface will again proceed by the Forster-Dexter mechanism²² involving the nonradiative decay of the exciton accompanied by the ionization of the metal. Both mechanism (d) and (e) are possible and plausible. To establish the dominant mechanism for extrinsic photoemission, we have studied the thickness dependence of the extrinsic photoemission yield from solid Xe.

Photoemission studies were conducted in the energy range 6–9.5 eV. The energy range 8.1–9.7 eV corresponds to excitation of bound excitons, being located below $E_{th} = 9.7$ eV. The vacuum ultraviolet light source consisted of a high pressure (2–5 atm) high intensity gas pulsed discharge lamp.²⁴ The light source emits a train of pulses, the pulse width being 2 μ sec, with a repetition rate which could be varied in the range 10–250 pulses sec^{-1} . The light was passed through a 0.3 m Czerny-Turner monochromator (McPherson 218) with a grating blazed at 1500 \AA , employing a spectral resolution of 5 \AA (0.025 eV). The monochromator was separated from the sample chamber by a LiF window. The optical arrangement allowed for a simultaneous measurement of optical absorption and photoemission yield. The emitter electrode consisted of a 3 mm wide gold strip evaporated on a LiF window. The collector electrode was a gold ring of 15 mm in diameter, located 30 mm from the emitter. The signal was amplified by a differential amplifier (Brookdeal-9432) followed by a low noise amplifier (Brookdeal-450) and finally amplified and integrated by a Boxcar integrator which was triggered by the same electrical pulse used for the lamp triggering. In this way a noise level of 5×10^{-18} A was achieved for the measurement of the photoelectric current. The samples were prepared by deposition of gaseous Xe (Matheson research grade) on the emitter electrode which was mounted on a variable temperature helium flow cryostat at 40 $^{\circ}$ K. This deposition temperature provides a well annealed sample. The films were deposited at the rate

of 50 $\text{\AA}/\text{min}$. The gaseous mixtures were prepared and handled in an ultrahigh vacuum system previously pumped down to less than 10^{-9} torr.

The film thickness d was determined from the measurement of the "oscillations" in the apparent transmittance of the Xe film deposited on the LiF holder in the spectral range above the onset of spectral absorption ($\lambda > 1600$ \AA). Measurements of d were conducted with visible light at $\lambda = 6600$ \AA and with vuv radiation at 1600 \AA . The film thickness was determined by counting the number M of wavelengths in the recorded spectrum vs time, which are given by $d = (M\lambda/2)(n^2 - \sin^2\theta)^{-1/2}$, where n is the refractive index ($n^2 = 2.23^{25}$) and θ is the angle of incidence. As is apparent from Fig. 1 d monitored at 6600 \AA exhibits a linear variation with the time of decomposition. d was further monitored by the same method at 1600 \AA yielding identical results. The accuracy of the determinations of d amounts to ± 10 \AA .

We have also measured the escape length L of electrons in pure solid Xe by monitoring the photocurrent from the gold emitter electrode in the spectral region 1600–1550 \AA where solid Xe is optically transparent. We expect the photocurrent i to be given by $i = i_0 \times \exp(-d/L)$. The results for several photon energies are displayed in Fig. 2. They exhibit two components, a fast initial drop of 30% from $d = 0$ to $d = 40$ \AA followed by an exponential decay of i and d . The short component is attributed to a primary surface coverage layer, which exhibits strong energy loss effects. It is possible that the first few layers of the film nucleate in a different configuration than the bulk. In the absence of structural data we cannot dwell further on this point. The long component results in $L = 850$ \AA , which is practically energy independent in the narrow energy range 7.7–8.0

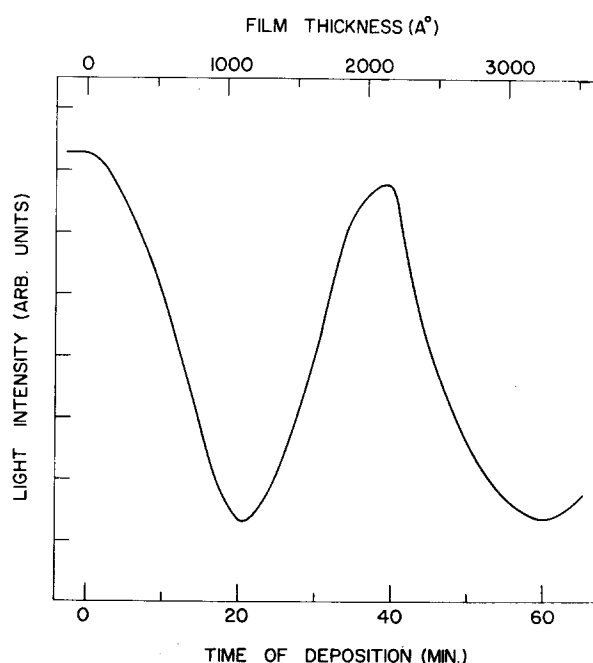


FIG. 1. Determination of the thickness of Xe films deposited on LiF as a function of the deposition time t , by the measurement of the optical interference bands in the apparent transmission at 6600 \AA .

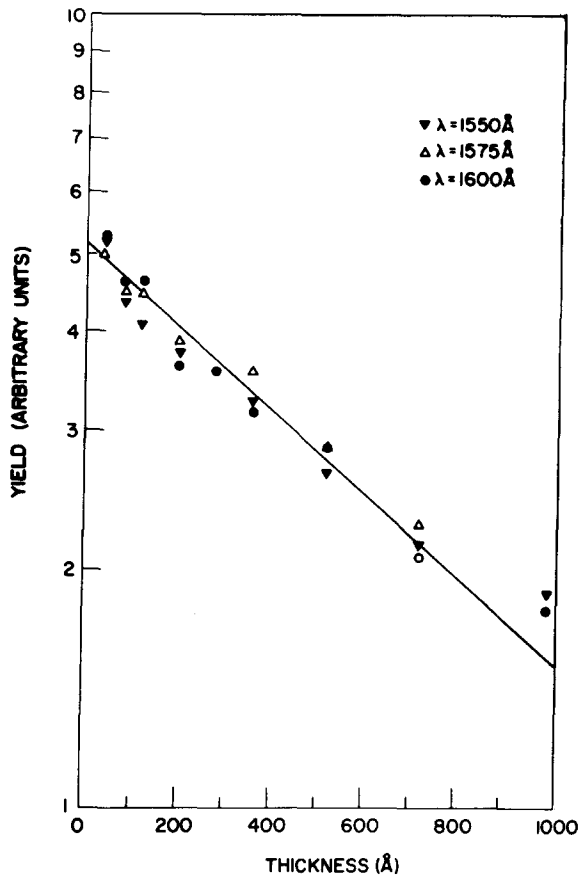


FIG. 2. A semilogarithmic plot of the photoemission current i from the gold emitter electrode (mounted on LiF) as a function of the thickness d of the Xe film. Data are presented for three values of the photon energies in the spectral range where solid Xe is optically transparent. The escape length L of the photoelectrons, which were ejected for the gold and escaped from the sample is obtained from the slope of the straight solid line according to $i = i_0 \exp(-d/L)$.

eV. This value for the escape length in solid Xe is comparable to the value $L = 1200 \text{ \AA}$ observed^{14c} in solid Ar. These values of L for solid rare gases are large compared to other materials.^{26b} In large gap insulators, the mechanisms of energy loss for electrons are inefficient allowing for a long mean free path of the hot electrons.

The extrinsic photoemission yield Y from solid Xe in the excitonic region 8.0–9.5 eV is portrayed in Fig. 3 for different values of the film thickness. We note that increasing d results in the attenuation of the photoemission from the pure gold. This effect cannot be wholly attributed to the trivial causes of optical absorption and reduction of the escape probability of the photoelectrons emitted via direct photon absorption by the gold because of two reasons. First, the energy dependence of Y exhibits pronounced peaks at the energies $n = 1$ ($^2P_{3/2}$) exciton located at 8.35 eV and for $n = 2$ ($^2P_{3/2}$) exciton located at 9.05 eV. Second, when these experimental data are corrected for optical absorption and for energy loss by the Xe film a finite extrinsic photocurrent, Y_e , results. Y_e is given by

$$Y_e = Y - Y_{Au}^0 \exp[-d(k + 1/L)] \quad (1)$$

and is displayed in Fig. 4. It was derived from the Y

values of Fig. 3 using the experimental values for the absorption coefficient,^{12,25,27} k , the relative values for photoemission from pure gold²⁸ Y_{Au}^0 , together with value $L = 850 \text{ \AA}$, which was assumed to be only weakly energy dependent through the whole energy range. An approximate estimate of the absolute values of Y_e was obtained using the absolute photoemission data for pure gold reported by Krolkowski and Spicer.²⁸

The central question we now face is whether the extrinsic photoemission can be described in terms of a long range dipolar interaction between a static localized excitation with the gold surface²⁹ or, alternatively, whether motion of "free" excitons has to be invoked for a proper interpretation of the data. Consider first the ET process induced by dipole-dipole coupling^{22,23} [mechanism (d)]. The rate of ET from a localized excitation separated by the distance $d_1 = (d - x)$ from the

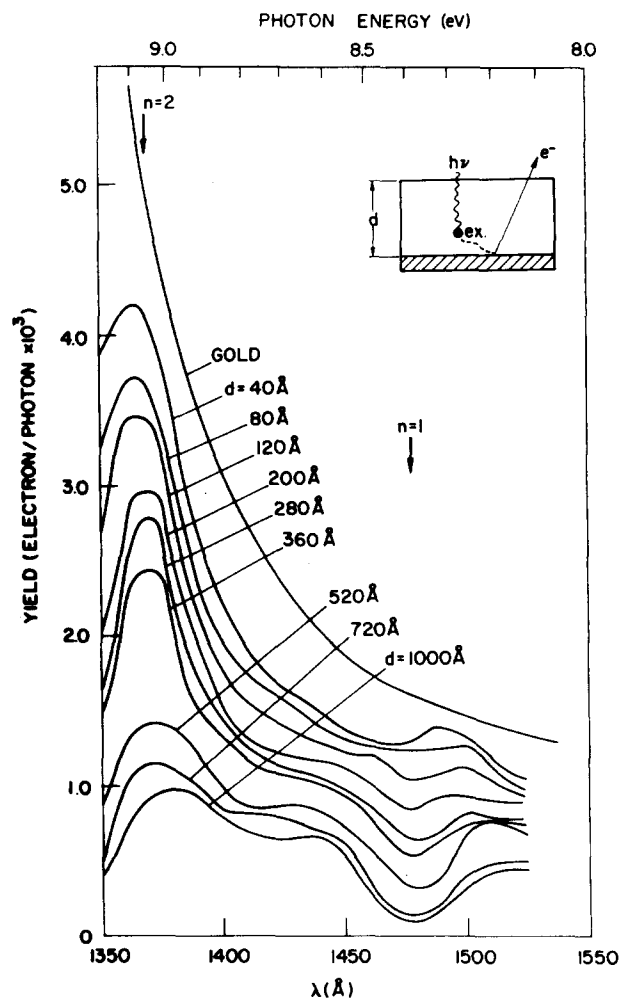


FIG. 3. Experimental photoemission yields $Y = i/I_0$ (where I_0 is the incident light intensity) from solid Xe deposited on the gold emitter electrode for various values of the Xe film thickness. The yield from the gold electrode (which is mounted on the LiF substrate) is also shown for comparison. The (approximate) absolute yields were obtained from the photoemission data for pure gold (Ref. 26). The positions of the $n = 1$ ($^2P_{3/2}$) and $n = 2$ ($^2P_{3/2}$) excitons of solid Xe are marked by arrows. The upper insert portrays schematically the extrinsic photoemission mechanism via "free" exciton diffusion to the gold followed by electron ejection from the electrode.

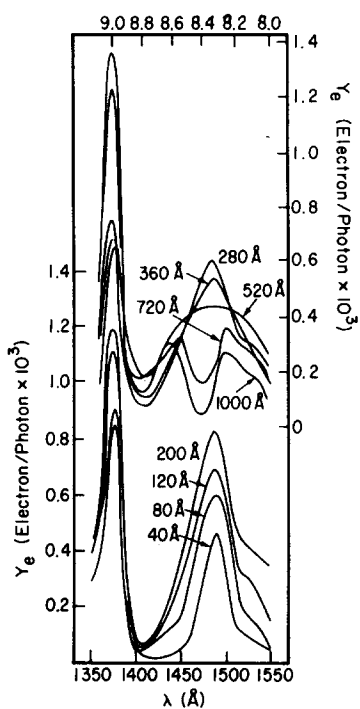


FIG. 4. Extrinsic photoemission yields Y_e for solid Xe films deposited on gold. The experimental yields were corrected according to Eq. (1) for hot electron emission from the gold via direct photon absorption. Left scale: yield data for $d=40, 80, 120,$ and 200 \AA . Right scale: yield data for $d=280, 360, 520, 720,$ and 1000 \AA .

surface to it, is

$$k_{\text{ET}}(d_1) = \eta/d_1^4 = \eta/(d-x)^4, \quad (2)$$

where the coefficient η is given in terms of Forster's theory²³ for the appropriate geometry. The photoemission yield is

$$Y_e = \int_0^d dx \frac{k k_{\text{ET}}(d-x) \exp(-kx)}{k_{\text{ET}}(d-x) + \tau_f^{-1}} \exp\left(\frac{-d}{L}\right), \quad (3)$$

where τ_f is the radiative lifetime of the diatomic rare gas molecule. Defining $d_0 = (\eta \tau_f)^{1/4}$ for an effective transfer radius we get for the ET mechanism

$$Y_e = k \exp\left(\frac{-d}{L}\right) \int_0^d \frac{\exp(-kx) dx}{1 + [(d-x)/d_0]^4}. \quad (4)$$

The experimental data for the d dependence of Y_e at 8.35 eV and at 9.05 eV could not be adequately accounted for by Eq. (4). While the low d range ($d \leq 200 \text{ \AA}$) could be fit with $d_0 = 150 \text{ \AA}$ the Y_e values for higher d (500–700 \AA) conforms to $d_0 = 300 \text{ \AA}$, thus the data for the d dependence of Y_e cannot be fit with a single value of d_0 and the discrepancy is a serious one.

We conclude that the dominating mechanism responsible for extrinsic photoemission in our system involves diffusion of "free" excitons to the gold surface. Invoking the diffusion model previously advanced by us in the study of exciton enhanced impurity photoionization¹⁴ the number density $n(x, t)$ of "free," mobile, excitons is governed by the diffusion equation.

$$\frac{\partial n(x, t)}{\partial t} = D \frac{\partial^2 n(x, t)}{\partial x^2} + k I_0 \exp(-kx) - \frac{n(x, t)}{\tau}, \quad (5)$$

where I_0 is the incident light intensity.

Under steady state conditions with the boundary conditions¹⁴ $n(0) = 0$ and $n(d) = 0$, Eq. (5) results in

$$n(x) = A \exp(-x/l) + B \exp(x/l) - C \exp(-kx), \quad (6a)$$

$$A = C[\exp(d/l) - \exp(-kd)]/[\exp(d/l) - \exp(-d/l)], \quad (6b)$$

$$B = C[\exp(-kd) - \exp(-d/l)]/[\exp(d/l) - \exp(-d/l)], \quad (6c)$$

$$C = I_0 k \tau / (k^2 l^2 - 1), \quad (6d)$$

$$l = (D\tau)^{1/2}. \quad (6e)$$

The extrinsic photoemission yield can be now expressed in terms of the exciton flux at $x = d$,

$$Y_e = \frac{1}{I_0} \left(-D \frac{\partial n}{\partial x} \right)_{x=d} \exp\left(\frac{-d}{L}\right) \quad (7)$$

which with the aid of Eq. (6) takes the following final form for the ED mechanism

$$Y_e = \frac{kl}{k^2 l^2 - 1} \left\{ \frac{2 - \exp(-kd)[\exp(-d/l) + \exp(d/l)]}{\exp(d/l) - \exp(-d/l)} - kl \exp(-kd) \right\} \exp(-d/L). \quad (8)$$

Our most reliable experimental data for Y_e span the energy range 8.0–8.6 eV of the lowest $n=1(2P_{3/2})$ exciton where our assumption concerning the energy independence of L can be quite safely applied. In this energy region the absorption coefficient varies in the range $(170 \text{ \AA})^{-1}$ (at 8.4 eV) and $(2200 \text{ \AA})^{-1}$ (at 8.0 eV). In Fig. 5 we portray the thickness dependence of Y_e analysed in terms of the diffusion model, Eq. (8). The agreement between theory and experiment for $l = 300 \text{ \AA}$ is excellent. On the basis of numerical calculations we assert that the deviations of the experimental data from the prediction of the ED model with $l = 300 \text{ \AA}$ amount to an uncertainty of 20% in the absolute value of l . In Fig. 6 we display the energy dependence of Y_e , which again exhibits good agreement with Eq. (8) for the same l value. It is gratifying that a single value of $l = 300 \text{ \AA}$ fits the data over a broad range of experimental parameters, i.e., $d = 40$ – 1000 \AA and $k^{-1} = 170$ – 2000 \AA , thus providing strong support for the extrinsic photoemission mechanism proposed herein.

The extrinsic photoemission yield in the energy range around 9.1 eV, corresponding to the $n=2(2P_{3/2})$ Wannier

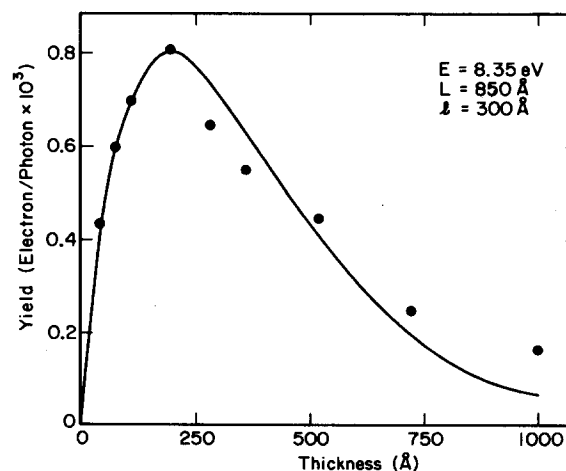


FIG. 5. The thickness dependence of the extrinsic photoemission yield at 8.35 eV. Open circles represent experimental data, while the solid curve was calculated from the diffusion model. Best fit obtained for $l = 300 \text{ \AA}$.

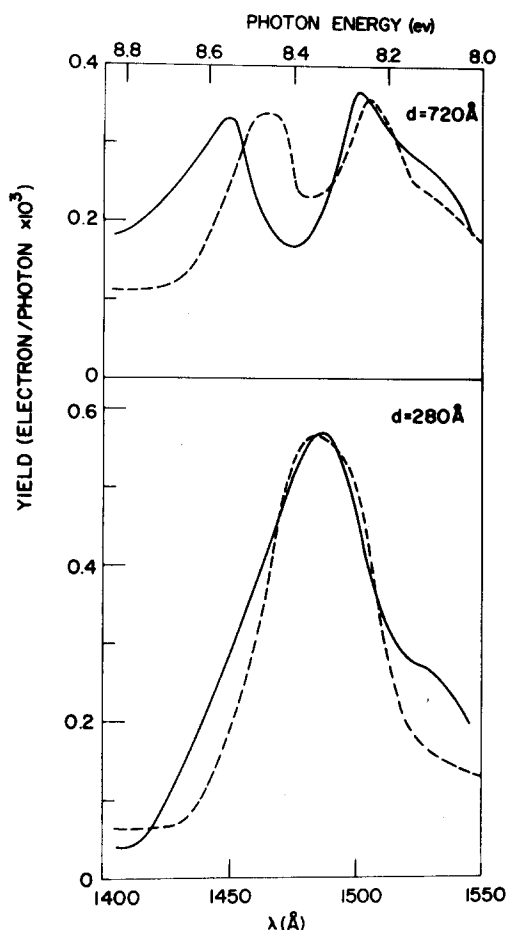


FIG. 6. The energy dependence of the extrinsic photoemission yield at constant d . Solid lines correspond to the experimental data, while the dashed curves correspond to the result of the diffusion model [Eq. (8)] with $l=300$ Å.

exciton in solid Xe, exhibits somewhat higher values of Y_e than expected on the basis of Eq. (8) with $l=300$ Å. It is tempting to conjecture that this excess extrinsic yield originates from $n=2$ excitons characterized by a higher diffusion length and which eject electrons at higher energy and thus with higher initial yield from the gold substrate. Such an interpretation would imply that the nonradiative $n=2 \rightarrow n=1$ multiphonon nonradiative relaxation process occurs on the time scale 10^{-12} – 10^{-11} sec, which is comparable to the lifetime of “free” mobile excitons. Extension of our studies will provide interesting information concerning radiationless electronic relaxation phenomena between exciton states in simple insulators.

The diffusion length $l=300$ Å for the “free” $n=1$ ($^2P_{3/2}$) exciton in solid Xe obtained from extrinsic photoemission studies lies within a numerical factor of 2 with the value¹⁴ $l=170$ Å previously obtained from exciton induced impurity photoemission in this system. It should be noticed that we have explicitly assumed that energy transfer occurs once the exciton reaches $x=d$. A more detailed examination of the long-range energy transfer process from the “free” exciton to the metal surface, which can occur over a distance of $d_0 \approx 100$ Å or so, will result in some lowering of l . Thus the agreement be-

tween the results of our previous work¹⁴ and the present data is as good as can be expected.

On the basis of the broad optical absorption linewidth, $\Gamma=0.16$ eV, of the $n=1$ ($^2P_{3/2}$) exciton²⁵ we argue that the “free” exciton in this system corresponds to the strong exciton–photon coupling limit^{1,9} and that lattice phonon relaxation “around” the exciton is efficient (on a time scale much shorter than τ). The exciton diffusion coefficient $D \approx 1$ cm² sec⁻¹ is estimated taking $\tau \approx 10^{-11}$ sec. For diffusive, incoherent exciton motion^{3b,8c} $D = M^2 a^2 / 6\hbar\Gamma$, where M is the transfer integral and $a=5$ Å corresponds to the internuclear spacing, resulting in $M \approx 0.2$ eV, which is reasonable.

In the present work we have presented rather detailed results for extrinsic photoemission from solid Xe. This phenomenon is, however, general and can in fact be encountered in any insulator where the exciton diffusion length is sufficiently large. In the case of solid rare gases other than solid Xe studied herein the following qualitative observations support the generality of this effect: (a) As we have already mentioned, extrinsic photoemission resulting from excitation in the exciton region was observed for Kr,^{14,16,17} Ar,^{14,17} and Ne.³⁰ (b) Photoelectron energy distribution studies for solid Ar induced by excitation in the energy range 12–12.6 eV reveal³¹ the appearance of an EDC peak near the vacuum level, similar to that observed from the pure gold substrate,²⁸ this component exhibits an enhancement (relative to the pure gold) at low d values (250 Å) and then decreases with increasing d . This result concurs with the proposed ED mechanism.

Finally, we would like to emphasize an important quantitative difference between the extrinsic photoemission in solid Ar, Kr, and Xe and that expected from solid Ne. In the former case efficient exciton trapping occurs and the “free” exciton lifetime is 10^{-12} – 10^{-11} sec, whereupon the diffusion length is relatively small. In the case of solid Ne exciton trapping does not take place and the optical emission exhibits the radiative decay of a “phonon dressed” free exciton.³² Thus in solid Ne the lifetime of the “free” exciton is $\sim 10^{-9}$ sec and the diffusion length will exceed by one order of magnitude the l value observed in solid Xe and in solid Ar. Dramatic extrinsic photoemission effects are expected in the excitonic series of moderately thick Ne films.

ACKNOWLEDGMENTS

This research was supported by the Nerken Foundation at the Tel-Aviv University and by the Deutsche Forschungsgemeinschaft DFG, at the Deutsches Elektronen-Synchrotron, Desy, Hamburg.

This research has been completed whilst one of us (J. J.) was on a Sabbatical leave at the Department of Physical Chemistry, Chemical Laboratory IV, The University of Copenhagen. The hospitality of Professor C. J. Ballhausen is gratefully acknowledged.

*Address during 1 September 1974–1 September 1975: Xerox Palo Alto Research Center, Palo Alto, California 94304.

†Address during 1 August–31 December 1974: Department of

- Physical Chemistry, Chemistry Laboratory IV, H. C. Ørsted Institute, University of Copenhagen, 2100 Copenhagen Ø, Denmark.
- ¹See for example (a) R. S. Knox, *Theory of Excitons* (Academic, New York, 1963); (b) S. A. Rice and J. Jortner, in *Physics and Chemistry of the Organic Solid State*, edited by F. Fox, M. Labes, and A. Weissberger (Interscience, New York, 1967), Vol. III, Chap. 4.
- ²O. H. Simpson Proc. R. Soc. A **238**, 402 (1957).
- ³(a) M. Levine, A. Szoke, and J. Jortner, J. Chem. Phys. **45**, 1591 (1966); (b) P. Avakian, V. Ernn, R. E. Merrifield, and A. Suna, Phys. Rev. **165**, 974 (1968).
- ⁴G. Gallus and H. C. Wolf, Z. Naturforsch. **23**, 1333 (1968).
- ⁵(a) R. C. Powell, Phys. Rev. B **2**, 1159 (1970); (b) R. C. Powell, Phys. Rev. B **4**, 628 (1971).
- ⁶V. L. Zima and A. N. Faidysh Opt. Spectrosc. **20**, 566 (1966).
- ⁷K. Uchida and M. Tomura, J. Phys. Soc. Jpn. **36**, 1358 (1974).
- ⁸(a) R. Bersohn and I. Isenberg, J. Chem. Phys. **40**, 3175 (1964); (b) J. Eisenger and R. G. Schulman, Proc. Natl. Acad. Sci. (U.S.) **55**, 1387 (1977); (c) M. Sommer and J. Jortner, J. Chem. Phys. **49**, 3919 (1968).
- ⁹Y. Toyozawa, Prog. Theoret. Phys. **20**, 53 (1958).
- ¹⁰The intermediate exciton in solid rare gases can be described (Ref. 1) either in terms of a modified Frenkel exciton where the tight binding picture has to incorporate large nonorthogonality-overlap connections or alternatively, in terms of a $n=1$ Wannier exciton subjected to large central cell connections.
- ¹¹(a) J. Jortner, L. Meyer, S. A. Rice, and E. G. Wilson, J. Chem. Phys. **59**, 5471 (1973); (b) N. G. Basov, M. Belashov, C. V. Bogdenkevich, V. A. Danilychev, and D. P. Khodkevich, J. Luminescence **1**, 834 (1970); (c) A. Gedanken, B. Raz, and J. Jortner, J. Chem. Phys. **59**, 5471 (1973); (d) A. Brodmann, R. Haensel, U. Hahn, U. Nielsen, and G. Zimmer, Vac. U. V. Radiation Phys. (to be published).
- ¹²I. T. Steinberger, C. Atluri, and O. Schnepf, J. Chem. Phys. **52**, 2723 (1970).
- ¹³We shall use the terms of "free" mobile excitons as distinct from trapped excitations. The "free" exciton in solid rare gases is medium-relaxed being strongly coupled to the medium phonons (Ref. 9). This excitation prevails prior to excitation trapping.
- ¹⁴(a) Z. Ophir, B. Raz, and J. Jortner, Phys. Rev. Lett. **33**, 415 (1974); (b) V. Saile, N. Schwentner, E. E. Koch, M. Skibowski, W. Steinmann, B. Raz, Z. Ophir, and J. Jortner, Vac. U. V. Radiation Phys. (to be published); (c) Z. Ophir, B. Raz, J. Jortner, V. Saile, N. Schwentner, E. E. Koch, M. Skibowski, and W. Steinmann, J. Chem. Phys. **62**, 650 (1975).
- ¹⁵From the analysis of the exciton induced photoemission in the C_6H_6/Xe system Ophir *et al.* [Ref. 14(a)] obtained $l/L=0.2$, where L for pure Xe was unknown and we took $L=350 \text{ \AA}$. Using the value $L=850 \text{ \AA}$ reported in present work we get $l=170 \text{ \AA}$.
- ¹⁶J. F. O'Brien and K. J. Teegarden, Phys. Rev. Lett. **17**, 919 (1966).
- ¹⁷N. Schwentner, M. Skibowski, and W. Steinmann, Phys. Rev. B **8**, 2365 (1973).
- ¹⁸I. T. Steinberger, E. Pantos, and I. H. Munro, Phys. Lett. A **47**, 299 (1974).
- ¹⁹S. I. Choi and S. A. Rice, J. Chem. Phys. **38**, 366 (1963).
- ²⁰E. Courtens, A. Bergman, and J. Jortner, Phys. Rev. **156**, 948 (1967).
- ²¹I. T. Steinberger, E. Pantos, I. H. Munro, and U. Asaf, Vac. U. V. Radiation Phys. (to be published).
- ²²(a) Th. Forster, Ann. Phys. (Leipzig) **2**, 55 (1948); (b) D. L. Dexter, J. Chem. Phys. **21**, 837 (1953).
- ²³M. Bucher, K. H. Drexhage, M. Fleck, M. Kuhn, D. Mobius, F. P. Schafer, J. Sondermann, W. Sperling, P. Tillmann, and J. Wiegand, Mol. Crystals **2**, 199 (1967).
- ²⁴Z. Ophir, B. Raz, U. Even, and J. Jortner, J. Opt. Soc. Am. (to be published).
- ²⁵G. Baldini, Phys. Rev. **128**, 1562 (1962).
- ²⁶(a) W. F. Krolikowski and W. E. Spicer, Phys. Rev. B **1**, 478 (1970); (b) I. Lindau and W. E. Spicer, J. Electron. Spectrosc. **3**, 409 (1974).
- ²⁷M. Skibowski (unpublished).
- ²⁸ Y_{Au}^0 was actually taken to be the photoemission yield from gold obtained from Fig. 1 by extrapolation of the straight line to $d=0$, accounting for primary surface coverage effects.
- ²⁹One can also consider in this context exciton (prior to excitation trapping) interacting with the metal. The formulation in both cases is identical.
- ³⁰E. E. Koch, V. Saile, N. Schwentner, and M. Skibowski, Chem. Phys. Lett. **28**, 562 (1974).
- ³¹N. Schwentner (to be published).
- ³²A. Gedanken, B. Raz, and J. Jortner, J. Chem. Phys. **59**, 1650 (1973).